Role of dynamical screening in excitation kinetics of biased quantum wells: Nonlinear absorption and ultrabroadband terahertz emission

Turchinovich, Dmitry; Monozon, B. S.; Jepsen, Peter Uhd

Published in:
Journal of Applied Physics

Link to article, DOI:
10.1063/1.2150256

Publication date:
2006

Document Version
Publisher's PDF, also known as Version of record

Role of dynamical screening in excitation kinetics of biased quantum wells: Nonlinear absorption and ultrabroadband terahertz emission

D. Turchinovich[a)]
Atom Optics and Ultrafast Dynamics, Debye Institute, Department of Physics and Astronomy, University of Utrecht, P.O. Box 80000, 3508TA Utrecht, The Netherlands

B. S. Monozon
Department of Physics, State Marine Technical University, Lotsmanskaya 3, 190008 St. Petersburg, Russia

P. Uhd Jepsen
Research Center COM, Technical University of Denmark, Building 345V, DK-2800 Kgs Lyngby, Denmark

(Received 16 May 2005; accepted 17 November 2005; published online 6 January 2006)

In this work we describe the ultrafast excitation kinetics of a biased quantum well, arising from the optically induced dynamical screening of a bias electric field. The initial bias electric field inside the quantum well is screened by the optically excited polarized electron-hole pairs. This leads to a dynamical modification of the properties of the system within an excitation pulse duration. We calculate the excitation kinetics of a biased quantum well and the dependency of resulting electronic and optical properties on the excitation pulse fluence, quantum well width, and initial bias field strength. Our calculations, in particular, predict the strongly nonlinear dependency of the effective optical absorption coefficient on the excitation pulse fluence, and ultrabroadband terahertz emission. Our theoretical model is free of fitting parameters. Calculations performed for internally biased InGaN/GaN quantum wells are in good agreement with our experimental observations [Turchinovich *et al.*, Phys. Rev. B **68**, 241307(R) (2003)], as well as in perfect compliance with qualitative considerations. © *2006 American Institute of Physics*. [DOI: 10.1063/1.2150256]

I. INTRODUCTION

The optical and electronic properties of a semiconductor quantum well (QW) subject to a transverse electric field are described in terms of the quantum confined Stark effect (QCSE).[1] The QCSE manifests itself as a decrease of the optical transition energy, which is a result of band-structure tilt. Application of a transverse electric field to a QW also leads to a spatial separation of the wave functions for the valence-band (VB) and conduction-band (CB) states, thus reducing the optical absorption coefficient and recombination rate. Apart from the material parameters, such as the QW and barrier band gaps, band offsets, electron and hole effective masses, and the QW width, the key parameter that defines the optical and electronic properties of the biased QW is therefore the bias field strength.

Absorption of a photon by a biased QW leads to the *instantaneous*, as opposed to the carrier dynamics in a bulk biased semiconductor (see e.g., Refs. 2 and 3), creation of a polarized electron-hole (e-h) pair as a result of the spatial separation of the VB and CB state wave functions. The electric field of such an optically created dipole has a polarity opposite to that of the bias field. Thus absorption of a photon by a biased QW leads to an instantaneous partial screening of the initial bias field. This will lead to a local microscopic modification of the optical and electronic properties of the system: The optical transition energy as well as the overlap between the VB and CB state wave functions will increase. The latter results in an enhancement of the optical absorption coefficient for the next photon to arrive. This makes optical absorption a strongly nonlinear process: The absorption condition for any given photon will completely depend on the cumulative screening action of all previously arrived photons.

The initial optical and electronic properties of the system will be restored when the excited e-h pairs have recombined and consequently the initial bias electric field has been restored.

Optically induced screening has already been observed, for example, in wurtzite-GaN-based QW structures under intense optical excitation. Such QW structures are subject to a strong internal bias electric field. This built-in electric field originates from the in-plane strain-induced piezoeffect due to the lattice mismatch between the QW and barrier materials and the spontaneous polarization of the wurtzite structure, and its strength can be as high as several MV/cm.[4–7] The main experimentally observed signature of optically induced screening is a blueshift in QW photoluminescence (PL) with an increase in excitation density, as it indicates the flattening of the band structure due to decrease of the bias field. This blueshift was observed, for example, in InGaN/GaN samples in intense cw excitation regime[8] and in AlGaN/GaN samples in intense nanosecond pulse excitation regime.[9] The static screening of the wurtzite-GaN-based QWs by the free carriers,[10] in particular, introduced by modulation doping,[11] was also studied theoretically.

Recently we have demonstrated that such an optically induced screening of a biased QW on a femtosecond time scale is best described as a discharge of a nanoscale capacitor within the duration of an excitation laser pulse.[12] In this pro-

[a)]Electronic mail: d.turchinovich@phys.uu.nl

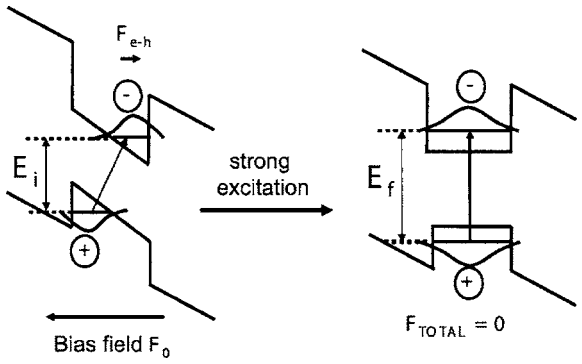

FIG. 1. Principle of the optically induced screening of a biased QW.

cess the electrostatic energy stored in the nanoscale capacitor is released in the form of an electromagnetic field transient due to the ultrafast polarization change. If the dynamical screening occurs on a femtosecond time scale then the spectral content of the transient will belong to the terahertz range. Our time-domain terahertz measurements were accompanied by time-integrated PL detection, which indeed showed the blueshift with an increase in excitation density.

Strong femtosecond excitation is the most efficient way to achieve partial or even complete optically induced screening of a biased QW, since a sufficient amount of polarized carriers can be created in a time interval much shorter than their recombination time, which is typically in the nanosecond range. After the excitation pulse is gone the system is left with modified optical and electronic properties (see Fig. 1). All the modifications of the optical and electronic properties of the QW take place *within* the duration of excitation pulse.

The dynamical screening effect thus plays an important (if not crucial) role in excitation kinetics of a biased QW. In order to describe the interaction of an ultrashort laser pulse with a biased QW, and to predict the resulting modification of its optical and electronic properties, it is therefore necessary to model the absorption process in a time-resolved manner.

Here we present a quantitative model to describe the excitation kinetics of a biased QW by an ultrashort laser pulse, where all the modifications of QW's optical and electronic properties take place within the duration of the laser pulse.

Based on the results of our calculations, which are free of phenomenological fitting parameters, we will be able to draw the fundamental conclusions about the role of dynamical screening in excitation kinetics of biased QWs.

II. THEORETICAL MODEL

In our theoretical model we consider the coherent interaction of the photon flux of the excitation laser pulse with the electronic structure of the biased QW.

We consider the case where only the ground states of the QW are excited at any time, and the energy of the incoming photons is always high enough to excite these states, both in initially fully biased and completely screened situations. The excitation laser pulse is defined by its duration, pulse shape, fluence, and the central wavelength, needed to calculate the number of photons in the laser pulse, which is described by its photon flux $\Phi(t)$.

We leave out any form of losses of the excited carriers from the QW within the duration of an excitation pulse. Typical processes leading to the loss of the excited carriers are recombination and tunneling (in case of multiple QWs), and they are normally much slower than the femtosecond pulse duration.

The main parameter describing the dynamical screening of a biased QW by optically created dipoles is *polarization dynamics*, and later we will arrive to the equation describing the temporal evolution of optically induced polarization—a key subject of our model.

The initial bias field F_0 of the QW is represented by an equivalent charge density N_0 spread over the QW interfaces,

$$F_0 = \frac{1}{\varepsilon\varepsilon_0} eN_0, \tag{1}$$

where N_0 is a sheet density and e is the elementary charge. This charge density is responsible for the initial polarization density P_0 of a biased QW, as it can be considered as a two-dimensional (2D) array of elementary dipoles (eL_z),

$$P_0 = N_0 eL_z = F_0 \varepsilon\varepsilon_0 L_z, \tag{2}$$

where L_z is the QW width.

Now we consider the compensation of this initial polarization density P_0 by the polarization density of optically excited e-h pairs. The e-h pair density is created with a rate of

$$r_{e\text{-}h} = \frac{dN_e}{dt} = \Phi(t)\alpha(t)L_z, \tag{3}$$

where N_e is a sheet density of excited carriers, and α is an optical absorption coefficient. The excited e-h pairs modify the polarization density P according to

$$\frac{dP}{dt} = ed(t)r_{e\text{-}h}(t), \tag{4}$$

where d is the effective separation between the excited electrons and holes in a QW, given by the distance between the mean weighted maxima of the wave functions of the empty CB and VB states, i.e., the states to be populated by an incident photon flux. In the following we will call these wave functions the "empty" wave functions. By combining Eqs. (3) and (4) we arrive to the equation describing the polarization dynamics in an optically excited biased QW,

$$\frac{dP}{dt} = ed(t)\Phi(t)\alpha(t)L_z. \tag{5}$$

The evolution of the total polarization density $P_t(t)$ inside a QW is then given by

$$P_t(t) = P_0 - \int_{-\infty}^{t} \frac{dP}{dt'}dt' = P_0 - eL_z \int_{-\infty}^{t} \Phi(t')\alpha(t')d(t')dt'. \tag{6}$$

This equation links the macroscopic polarization of the sys-

tem, *coherently* induced by a photon flux $\Phi(t)$, to the microscopic properties of the QW, and describes the main subject of our model.

In principle, Eq. (6) can be further reduced to the treatment involving the interaction of electric field in the laser pulse and the phenomenological effective time-dependent (vanishing) nonlinear susceptibility.[13] But we would like to emphasize that *photon flux* treatment is absolutely essential within the framework of our model, since it is the temporal intensity profile of the excitation pulse which provides an account over density of excited e-h pairs.

The absorption coefficient $\alpha(t)$ and the effective separation between the excited electrons and holes $d(t)$ are defined by the electric field $F(t)$ inside the QW. This electric field is the key dynamical parameter needed to calculate the wave functions and eigenenergies of the QW. The absorption coefficient of the biased QW can be described as

$$\alpha(t) = \alpha_{\max} M^2(t), \tag{7}$$

where $M(t)=\langle \psi_e(t) | \psi_h(t) \rangle$ is the time-varying overlap integral of the empty wave function ψ_e and ψ_h of the CB and VB states, and $\alpha_{\max}$ is the absorption coefficient of an unbiased QW, i.e., the QW with a maximal wave-function overlap. As the polarization inside the QW changes due to the optically induced screening, the empty wave functions are modified. At each step in time we use the following effective field:

$$F(t) = \frac{1}{\varepsilon \varepsilon_0 L_z} P_t(t), \tag{8}$$

to calculate the empty wave functions ψ_e and ψ_h and electron and hole eigenenergies $E_{e,h}$ solving the Schrödinger equation for a uniformly biased QW with infinite barriers,

$$-\frac{\hbar^2}{2m_j}\frac{d^2\psi_j(z,t)}{dz^2} + q_j F(t) z \psi_j(z,t) = E_j(t)\psi_j(z,t), \tag{9}$$

where $j=e$ and h, $m_{e,h}$ are the electron and hole effective masses, z is the transverse coordinate of the QW, $q_{e,h}=\mp e$, and the electric field $F(t)$ is directed perpendicular to the QW interfaces positioned at $z=\pm L_z/2$. The wave functions satisfy the condition $\psi_j(\pm L_z/2, t)=0$. The variational method developed originally by Bastard *et al.*[14] was used to solve Eq. (9), as it allowed us to obtain the wave functions and eigenenergies in the weak, intermediate, and strong electric-field regimes continuously, thus providing the continuous temporal dependencies of calculated parameters. This continuity is required for the calculation of the terahertz emission resulting from the rapid polarization change.

The initial conditions to solve Eq. (6) and therefore to obtain the key optical and electronic parameters $P_t(t)$, $F(t)$, $\psi_{e,h}(t)$, $\alpha(t)$, $d(t)$, and $r_{e\text{-}h}(t)$ are $F(-\infty)=F_0$, $M(-\infty)=\langle \psi_e | \psi_h \rangle_{F=F_0}$, and $\Phi(-\infty)=0$.

It should be noted here that the two approximations have been made in the above treatment. Firstly, in the calculation of the optically induced polarization we assumed that the electrons and holes excited by the given portion of the photon flux are localized exactly under the centroids of their corresponding empty wave functions. This assumption has been demonstrated to be accurate in Ref. 15, where the experimental and calculated optically induced polarizations created in the QW with a variable bias field under a very weak nonscreening excitation have demonstrated a perfect agreement. Secondly, we introduced the effective uniform electric field inside the QW at all times, in a similar manner as in Ref. 16. In general, the electric field in the biased QW in the presence of the screening charge carriers is nonuniform and is given by the distribution of the carriers under their corresponding wave functions. But as was shown in Ref. 10, the electric field in the strongly biased QW is nearly uniform in a very broad range of the screening carrier densities, and the nonuniformity is only pronounced when the QW approaches the point of complete screening.

The above approximations by no means influence the general nature of the dynamical screening effect. As will be shown below, our calculations demonstrate a rather decent agreement with the available experimental data.

III. RESULTS AND DISCUSSION

Here we present the results of the calculations based on the material parameters of InGaN/GaN QWs, widely used in experiments. As discussed above, this type of the QWs has very strong internal bias electric field with reported values of 1.6 and 3.1 MV/cm at the indium concentrations of 12% and 22% in the QW material, respectively, for the QWs with a typical width of a few nanometers.[7] The effective masses of the carriers are $m_e=0.2m_0$ and $m_h=2.0m_0$ (Ref. 7) for the electrons and holes, respectively, where m_0 is the free-electron rest mass. The maximum absorption coefficient $\alpha_{\max}$ was chosen to be that of GaN at the absorption edge, $\alpha_{\max}=1.2\times10^5\ \mathrm{cm}^{-1}$.[17] The static dielectric constant is $\varepsilon=10.28$.[18] We assume a Gaussian temporal profile of the excitation laser pulse with a full width at half maximum (FWHM) duration of 100 fs, centered at $t=0$ fs. The incident photon energy is assumed to be 3.1 eV, corresponding to a central wavelength of 400 nm. We consider excitation pulse fluences in the range between 0 and 1.5 mJ/cm^2. These parameters are typical for the frequency-doubled Ti:sapphire regenerative amplifier used in our experiments on ultrafast optical screening of InGaN/GaN QWs.[12]

In Figs. 2–4 the temporal evolution of the empty wave functions and the temporal and spatial profile of the e-h density creation rates are shown for a QW with a bias field of 3 MV/cm and $L_z=2.5$ nm, which is subject to excitation at various pump fluences. The wave functions and e-h density creation rate dynamics clearly differ in dependence on the pump fluence.

In Fig. 2(a) at the excitation fluence of 0.15 mJ/cm^2 the wave functions are only slightly modified by the excited carriers, since at this weak excitation no substantial screening is achieved. As a result, the electrons and holes are created in strongly spatially separated states within the time range of the excitation pulse [Fig. 2(b)]. The displacement of the hole wave functions from the center of the QW is stronger than

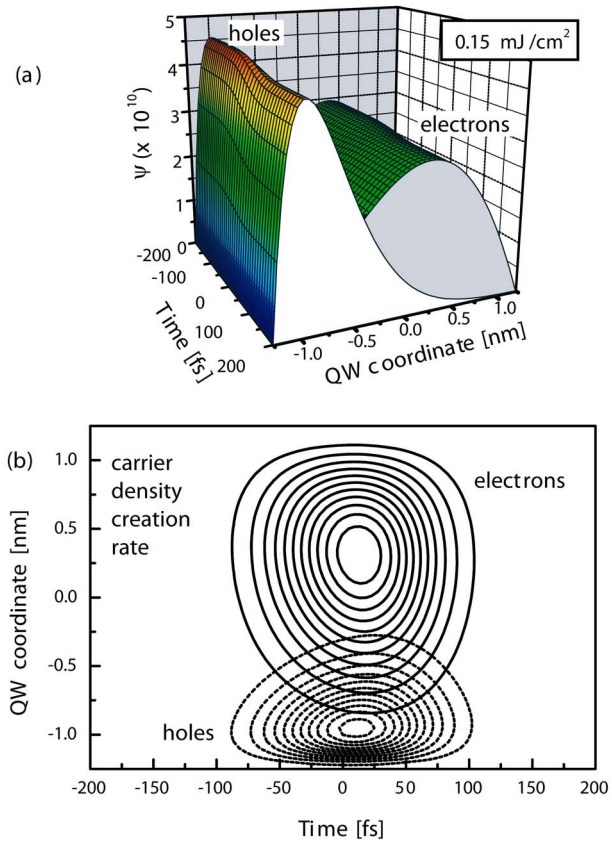

FIG. 2. (Color online) (a) Temporal evolution of "empty" wave functions and (b) temporal and spatial evolution of carrier density creation rate in the QW with $F_0=3$ MV/cm and $L_z=2.5$ nm subject to 100 fs excitation with a fluence of 0.15 mJ/cm^2.

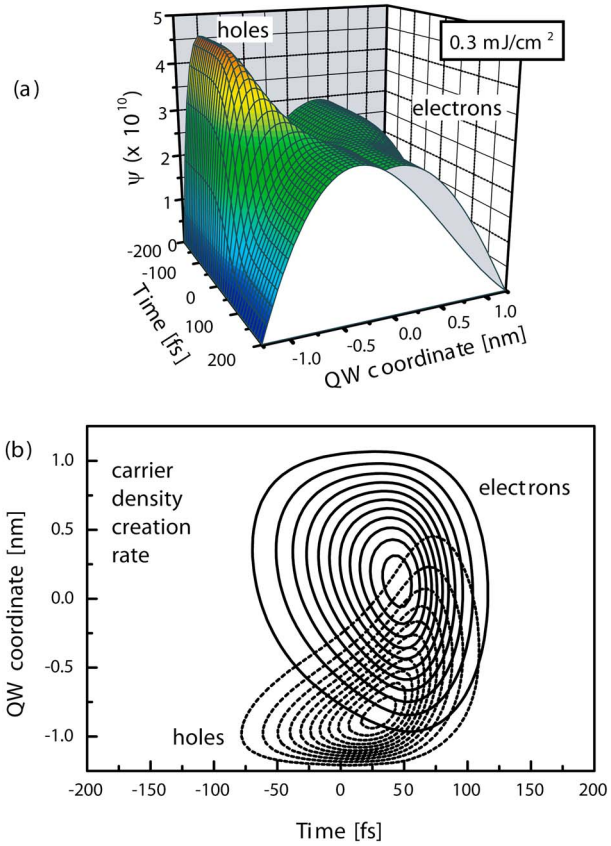

FIG. 3. (Color online) (a) Temporal evolution of "empty" wave functions and (b) temporal and spatial evolution of carrier density creation rate in the QW with $F_0=3$ MV/cm and $L_z=2.5$ nm subject to 100 fs excitation with a fluence of 0.3 mJ/cm^2.

that of the electrons due to the larger effective mass of the holes. This weak-pump picture well describes the experiment from work.[15]

With increase in the excitation pulse fluence to 0.3 mJ/cm^2 [see Fig. 3(a)] a strong dynamical modification of empty wave functions is demonstrated, indicating the substantial (but not yet complete) screening of the initial bias field. The evolution of the e-h density creation rate demonstrates strong dynamics [see Fig. 3(b)]. Interestingly, in this case the maximum of the e-h density creation rate is found after the incident photon flux reached its maximum. This phenomenon has a general fundamental nature and will be discussed below.

At a relatively high pulse fluence of 0.85 mJ/cm^2 [Figs. 4(a) and 4(b)] a complete screening of the QW is achieved within the duration of the excitation pulse. The empty wave functions of electrons and holes move rapidly towards the middle of the QW and at a certain point the electrons and holes are created in unpolarized states. The complete screening is achieved even before the incident photon flux has reached its maximum.

The temporal evolution of the effective bias electric field inside the QW, the absorption coefficient, and the e-h density creation rate are shown in Figs. 5(a)–5(c), for the three excitation fluences used in Figs. 2–4. The normalized photon flux of the laser pulse $\Phi(t)$ is also shown in the figure.

For all the three excitation fluences the initial absorption coefficient is rather small as defined by the small initial wave-function overlap. At weak excitation fluence of 0.15 mJ/cm^2 no significant bias field screening is achieved, and therefore no significant enhancement of the absorption coefficient is observed. Therefore the maximum of the e-h density creation rate is found at $t=10$ fs, slightly later than the maximum of the incident photon flux. The total sheet density of the excited e-h pairs, given by $N_{\text{total}}=\int_{-\infty}^{+\infty} r_{e\text{-}h}dt$, is also small.

With an increase in the excitation pulse fluence to 0.3 mJ/cm^2 the substantial screening process continues throughout the duration of the excitation pulse, and $r_{e\text{-}h}$ peaks at around 50 fs. This is much later than the maximum of the incident photon flux. The absorption coefficient is strongly enhanced at later times due to substantial bias field screening, and consequently larger empty wave-function overlap. Therefore the e-h density creation rate also finds its maximum at large positive time delay.

At strong excitation of 0.85 mJ/cm^2 the QW is completely screened already on the leading edge of the excitation pulse, at around -10 fs, therefore the absorption coefficient also reaches its maximum at around -10 fs. However, since the incident photon flux still increases and reaches its maximum at exactly $t=0$, the maximum e-h pair creation rate is also found at $t=0$.

Based on the previous discussion, we note that in general $r_{e\text{-}h}$ [see Eq. (3)] will be largest at $t\geqslant 0$ in case of a tempo-

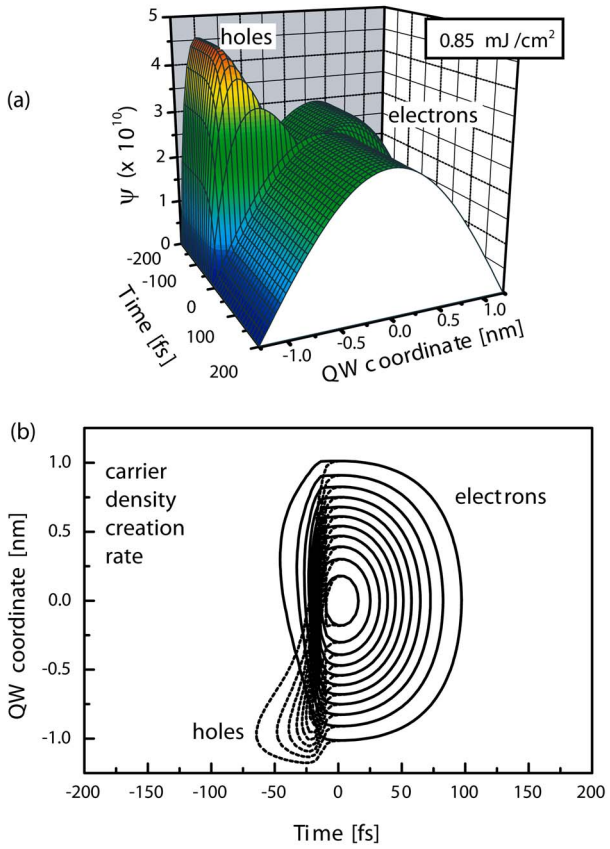

FIG. 4. (Color online) (a) Temporal evolution of "empty" wave functions and (b) temporal and spatial evolution of carrier density creation rate in the QW with F_0=3 MV/cm and L_z=2.5 nm subject to 100 fs excitation with a fluence of 0.85 mJ/cm^2.

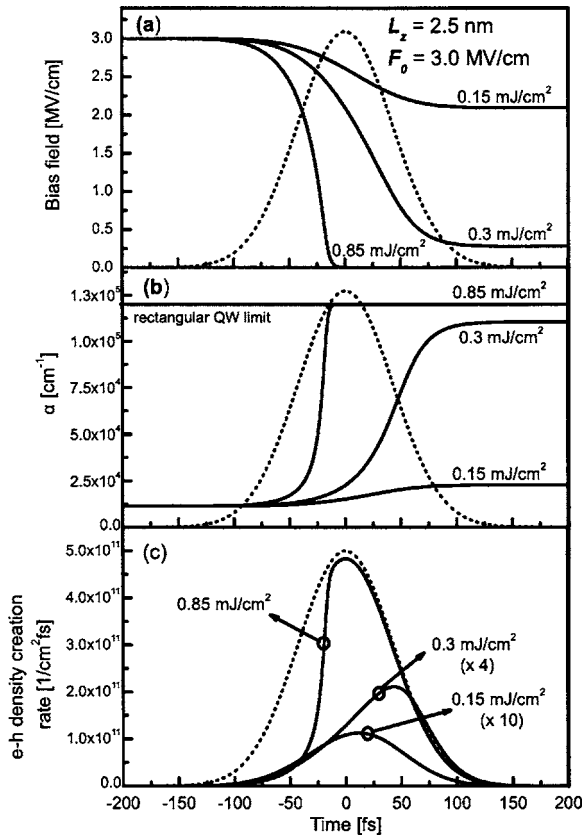

FIG. 5. Temporal evolution of (a) a bias electric field in a QW, (b) absorption coefficient, and (c) of e-h density creation rate for a QW with L_z =2.5 nm and F_0=3 MV/cm excited with the laser pulses of 0.15, 0.3, and 0.85 mJ/cm^2 fluence (solid lines). Normalized temporal shape of the photon flux in the excitation pulse (dashed line).

rally symmetrical excitation pulse. It will find its maximum at t=0 if the complete screening is reached on the leading edge of the excitation pulse or exactly at it maximum. In the case, when no complete screening is achieved or if the complete screening is achieved on the trailing edge of the excitation pulse $r_{e\text{-}h}$ will find its maximum at $t>0$. In the limiting cases of (i) a very weak excitation, where the screening effect is negligible and of (ii) a very strong excitation, where the complete screening of the bias field is reached within the very first moments of the excitation pulse duration, the e-h density creation rate will follow the temporal shape of the incident photon flux. In the case of the very weak excitation it will be given by $r_{e\text{-}h}^{\text{weak}}=\alpha_{\max}M^2_{[F=F_0]}\Phi(t)L_z$, and in the case of the very strong excitation it will have a form of $r_{e\text{-}h}^{\text{strong}}=\alpha_{\max}\Phi(t)L_z$.

Now we present the dependencies of resulting optical and electronic parameters, mainly observed in experiments, on the excitation fluence for QWs with different widths and initial bias field strengths.

In Figs. 6(a), 6(b), 7(a), and 7(b) we show the resulting effective bias field in the QW, the resulting Stark shift in the PL spectrum in dependence of the excitation fluence for QWs with L_z=1.5, 2, and 2.5 nm and the initial bias field strengths of 1.5 and 3 MV/cm. These QW parameters are typical for wurtzite InGaN/GaN QWs experimentally studied in the literature.[7,8,12,19]

Interestingly, the dependencies of the resulting Stark shifts and effective bias fields in the QWs on the pump fluence [see Figs. 6(a), 6(b), 7(a), and 7(b)] do not always show unambiguous trend with the initial potential drop across the QW (and therefore the initial wave-function separation). The QWs with initially greater wave-function overlap do not necessarily reach screening at weaker excitation fluences. This once again demonstrates the strong nonlinearity of the excitation kinetics of a biased QW. For example, the thicker QW at some point can provide more excited e-h pairs separated by a larger distance, and thus the screening process will be sped up in comparison with a narrower QW.

In the inset of Fig. 7(b) we show a comparison between the calculated Stark shifts for the QWs with an initial bias of 3 MV/cm and L_z of 2.0 and 2.5 nm and those measured in $In_{0.2}Ga_{0.8}N$/GaN QWs with an initial bias of 3.1 MV/cm and the L_z of 1.8 and 2.7 nm (experimental data taken from Refs. 12 and 20).

Our calculations, free of any fitting parameters, are in good agreement with the experimental results, demonstrating that the assumptions used in our theoretical model are well justified.

As was shown above [see Figs. 5(b) and 6(b)], depending on the excitation fluence, the absorption coefficient can undergo dramatic enhancement within the excitation pulse duration. Here we introduce an effective absorption coefficient, calculated as

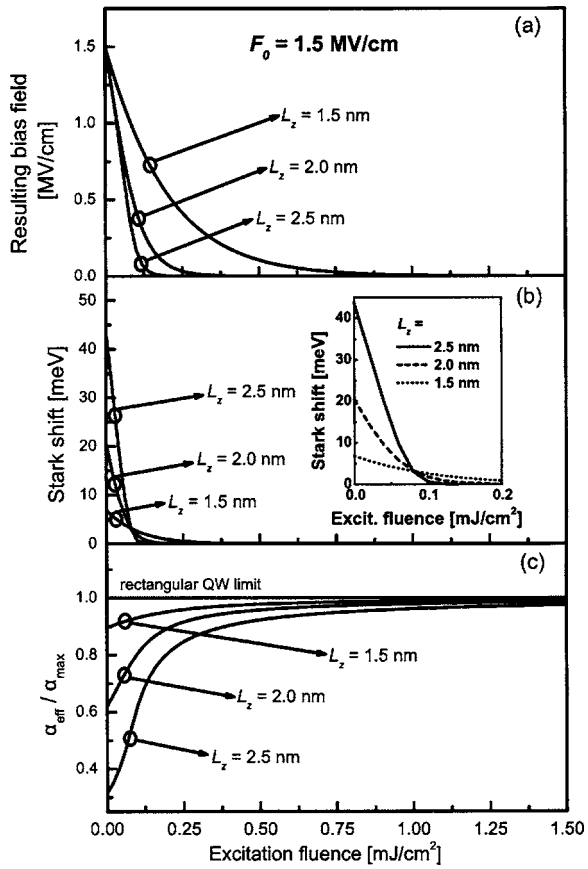

FIG. 6. (a) The resulting effective electric field in the QW, (b) Stark shift in the PL, and (c) ratio $\alpha_{\text{eff}}/\alpha_{\max}$ vs excitation fluence for a QW with F_0 =1.5 MV/cm and the L_z of 1.5, 2, and 2.5 nm. Inset of (b): Stark shifts for these QWs shown on magnified excitation fluence scale. Excitation pulse duration is 100 fs.

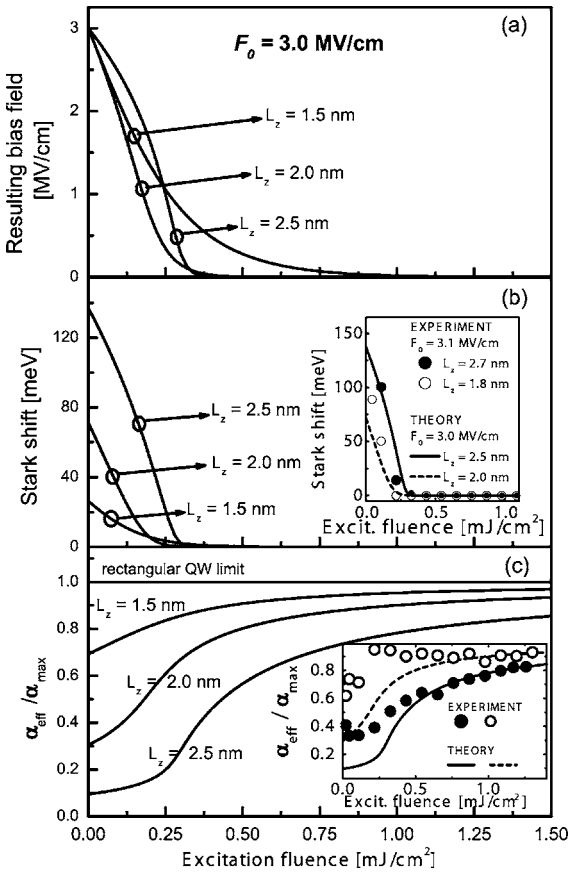

FIG. 7. (a) The resulting electric field in the QW, (b) Stark shift in the PL, and (c) ratio $\alpha_{\text{eff}}/\alpha_{\max}$ vs excitation fluence for a QW with F_0 =3.0 MV/cm and the L_z of 1.5, 2, and 2.5 nm. Inset of (b): Calculated excitation fluence dependency of Stark shift in the PL for the QWs with F_0=3 MV/cm and L_z of 2.0 nm (dashed line) and 2.5 nm (solid line); and measured Stark shifts for the QWs with F_0=3.1 MV/cm and L_z of 1.8 nm (open circles) and 2.7 nm (full circles). Inset of (c): Calculated excitation fluence dependency of ratio $\alpha_{\text{eff}}/\alpha_{\max}$ for the QWs with F_0=3 MV/cm and L_z of 2.0 nm (dashed line) and 2.5 nm (solid line), and experimental measure for α_{eff} for the QWs with F_0=3.1 MV/cm and L_z of 1.8 nm (open circles) and 2.7 nm (full circles). Excitation pulse duration is 100 fs in both theory and experiment.

$$\alpha_{\text{eff}} = \frac{1}{L_z}\frac{\int_{-\infty}^{+\infty} r_{e\text{-}h}(t)dt}{\int_{-\infty}^{+\infty}\Phi(t)dt}. \tag{10}$$

α_{eff} is essentially the absorption coefficient of a QW in a static "linear" representation, i.e. as measured in a time-integrated experiment. At zero excitation fluence $\alpha_{\text{eff}} = \alpha_{\max}(M^2_{[F=F_0]}/M^2_{\max})$, where $M_{\max}=1$ in an infinite unbiased QW.

In Figs. 6(c) and 7(c) the ratios $\alpha_{\text{eff}}/\alpha_{\max}$ are shown. The dependency of the effective absorption coefficient on excitation fluence is strongly nonlinear.

The wider wells show more dramatic enhancement of the effective absorption coefficient around the excitation fluence at which the total screening is reached. In the samples with smaller initial potential drop across QW the effective absorption coefficients are higher due to easier screening conditions, and their recovery occurs at lower excitation fluence. At higher excitation fluences α_{eff} tends to the value of $\alpha_{\max}$, as expected from qualitative considerations.

The nonlinear behavior of effective absorption is also confirmed in the experiment. The ratio of spectrally and temporally integrated PL intensity to the excitation fluence $\int_\omega\int_t I_{\text{PL}}(\omega,t)d\omega dt/\int_{-\infty}^{+\infty}\Phi(t)dt$ is a measure of the effective optical absorption within the framework of our model [see Eq. (10)], assuming that the nonradiative recombination can be neglected.

In the inset of Fig. 7(c) we compare our calculations of effective absorption coefficients with the ratios of experimental spectrally and temporally integrated PL to the excitation fluence taken from Refs. 12 and 20. The experimental dependencies were individually normalized to the maxima of the corresponding theoretical curves, since the PL intensity was measured in arbitrary units, and the PL collection efficiency also differed from sample to sample. We observe a rather decent agreement between our parameter-free calculations and experimental data, especially at higher excitation fluence.

As was discussed above, screening of a biased QW on an ultrafast time scale results in a rapid polarization change. This polarization change will lead to the emission of an electromagnetic field transient with terahertz frequency content, thus releasing the electrostatic energy initially stored in the biased QW, which is a nanoscale capacitor.[12] The temporal

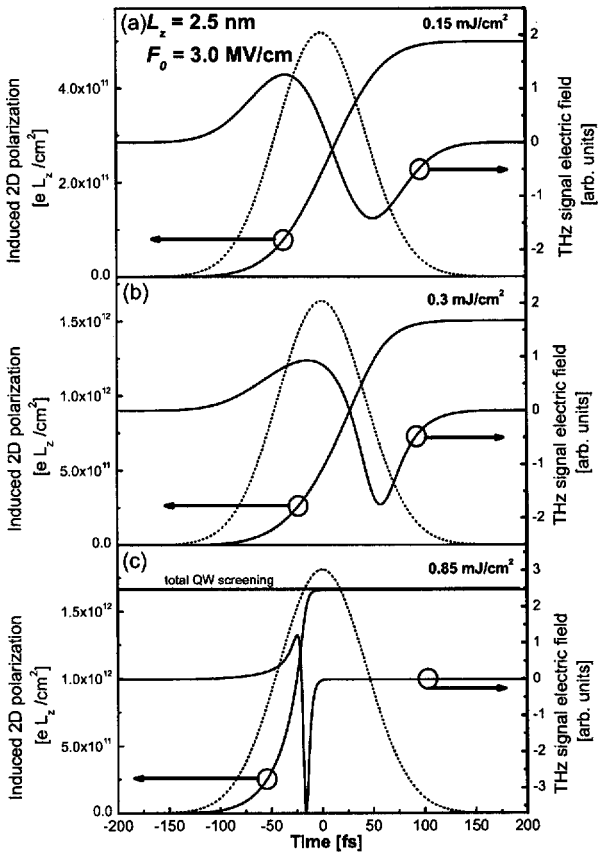

FIG. 8. Temporal evolution of induced 2D polarization and electric-field strength of the emitted terahertz transient for a QW with F_0=3 MV/cm and L_z=2.5 nm, excited with a 100 fs pulse of (a) 0.15 mJ/cm^2, (b) 0.3 mJ/cm^2, and (c) 0.85 mJ/cm^2 fluences. Normalized temporal shape of the photon flux in the excitation pulse (dashed line).

evolution of the electric field of the terahertz transient in the far field is given by the second temporal derivative of the induced polarization (see, for example, Refs. 15 and 21).

In Fig. 8 we show the screening-induced polarization dynamics and the far-field temporal shape of the emitted terahertz transient for a QW with an initial bias field of 3 MV/cm and L_z=2.5 nm excited by a laser pulse with the fluences of 0.15, 0.3, and 0.85 mJ/cm^2. The temporal shape of an excitation pulse is also shown in the figure. The induced polarization is shown in units of equivalent elementary dipoles (eL_z) per unit area. The initial polarization given by the bias electric field and the QW width is in this case of $-1.66\times10^{12}eL_z$ cm^{-2}. It is negative, because we assume the bias field to be directed against the z axis.

In the case of weak (0.15 mJ/cm^2) excitation fluence [Fig. 8(a)] the screening effect is small and the induced polarization change is also small. The temporal shape of the induced polarization therefore resembles that of the integral of the incident flux. In the case of stronger excitation fluence of 0.3 mJ/cm^2, as shown in the Fig. 8(b), substantial screening is achieved on the trailing edge of the laser pulse, and the resulting induced polarization is stronger and its dynamics is somewhat faster. This results in a faster and temporally asymmetric terahertz pulse. In the case of total screening of the QW already on the leading edge of the 0.85 mJ/cm^2 excitation pulse [see Fig. 8(c)] the induced polarization fully

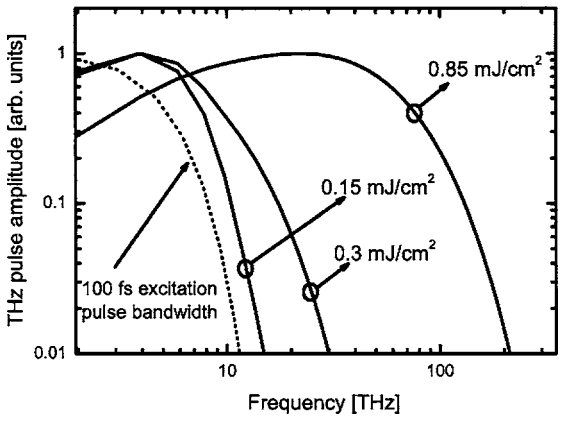

FIG. 9. Normalized frequency spectra of terahertz transients emitted from a QW with F_0=3 MV/cm and L_z=2.5 nm, excited with a pulse of 0.15 mJ/cm^2, 0.3 mJ/cm^2, and 0.85 mJ/cm^2 fluences. The spectra are plotted on a log-log scale.

compensates that of the initial bias already at a negative time. The emitted terahertz pulse shows very fast features, and its duration is considerably shorter than that of an excitation pulse, reaching well into near infrared.

In Fig. 9 we show the normalized frequency spectra of these terahertz transients on a double logarithmic scale. Dramatic spectral broadening is observed with increasing excitation fluence. The excitation pulse bandwidth is the lowest limit for the bandwidth of the terahertz transients emitted within the duration of the excitation pulse. In the case of weak excitation the spectrum of the emitted terahertz transient is only slightly broader than that of the excitation pulse. With an increase of the excitation fluence we observe considerable spectral broadening, and at 0.85 mJ/cm^2 excitation the spectral bandwidth of the emitted pulse is already approximately 20 times higher than that of the excitation pulse.

Generation of ultrabroadband terahertz radiation in a biased QW is quite understandable. Since the total screening of the biased QW can be reached in a time interval much shorter than the duration of the excitation pulse, and thus all the stored electrostatic energy of the biased QW will also be released faster. This leads to an important consequence: Within the framework of our model the spectral bandwidth of the terahertz pulse emitted as a result of dynamical screening of the QW by a short laser pulse will *always* (i) exceed that of the excitation pulse, and (ii) grow with increasing excitation fluence (which may be very promising for broadband terahertz spectroscopy applications), but the total pulse energy will still be limited by that initially stored in the biased QW.

This is in striking contrast with the terahertz emission resulting from below-band-gap optical rectification in a nonlinear crystal where the terahertz pulse is also emitted within the duration of an excitation pulse. The optical rectification technique allows for the conversion of the excitation pulse bandwidth into that of the emitted terahertz pulse, and is known to generate the fastest terahertz pulses up to date.[22] In this case the terahertz pulse duration and bandwidth are limited by that of the excitation pulse, whereas the energy of the emitted terahertz transient grows quadratically with increasing excitation fluence (see, for example Ref. 23).

The spectral broadening discussed in this paper was not observed in our recent experiment[12] due to a common experimental limitation: Detection of terahertz pulses with a bandwidth exceeding that of the excitation laser pulse is impossible with the conventional terahertz time domain spectroscopy (TDS) approach, because both generation and sampling of the temporal shape of the terahertz pulse are performed with the laser pulses of the same duration. This restricts the bandwidth of the detected terahertz pulse to that of the excitation laser pulse. The spectral broadening effect may be verified in a terahertz-TDS experiment using a temporally stretched excitation pulse and a short detection pulse.

IV. CONCLUSIONS

We have shown that the excitation kinetics of a biased QW is dominated by the dynamical screening of the bias electric field inside the QW, and have developed a time-resolved model to describe this process. This model contains no fitting parameters, and can be applied to the calculation of screening dynamics in QW structures independent of material and initial bias electric field, given that the excitation pulse is much faster than the recombination time of the carriers in the QW, that the energy of the photons in the excitation pulse is always high enough to excite the e-h pairs in the QW in both initially biased and completely screened states, and that the joint density of states in a QW provides enough e-h pairs to be excited within the bandwidth of an excitation pulse. Apart from the material parameters of the QW structure and initial bias electric-field strength the input parameter used for the calculations is the incident photon flux.

We have shown that within the duration of the excitation pulse the key optical and electronic parameters of the QW such as the effective bias electric field, absorption coefficient, optical transition energy, and electron-hole density creation rate can undergo dramatic modification as a result of the strongly nonlinear dynamical screening of the initial bias electric field by that of the optically created polarized electron hole pairs. At strong excitation total screening of the biased QW can be reached on a time scale much shorter than the excitation pulse duration.

Although relatively simple but containing no fitting parameters, our model turns out to be quite accurate: The calculated dependencies of the resulting Stark shift in the PL spectra and the effective absorption coefficients for the QWs with a bias field of 3 MV/cm show very good agreement with those experimentally measured by us in similar structures.[12,20]

Any other more elaborate (and therefore more resource consuming) approach to calculate the band structure of the QW in the presence of screening charges (see, for example, Refs. 10, 11, and 16) can be used within the main frame of our model. We note the general similarity between the results of our time-resolved calculations and the static calculations presented in the above-cited works.

In this work we have demonstrated the fundamental nonlinearity of the excitation kinetics of a biased QW due to dynamical screening effect. Perhaps the most intriguing prediction of our model is that an extremely short terahertz transient with a bandwidth significantly exceeding that of the excitation pulse will be generated at strong excitation of the biased QW.

These phenomena may be of high interest for modern optoelectronic applications, such as ultrafast switches, optical limiters, and ultrabroadband terahertz spectrometers.

ACKNOWLEDGMENTS

We would like to acknowledge many stimulating discussions with Hanspeter Helm, Jaap Dijkhuis, and Jørn Hvam.

[1] D. A. B. Miller, D. S. Chemla, T. C. Damen, A. C. Gossard, W. Wiegmann, T. H. Wood, and C. A. Burrus, Phys. Rev. Lett. **53**, 2173 (1984).
[2] A. Leitenstorfer, S. Hunsche, J. Shah, M. C. Nuss, and W. H. Knox, Phys. Rev. Lett. **82**, 5140 (1999).
[3] A. Schwanhäußer, M. Betz, M. Eckardt, S. Trumm, L. Robledo, S. Malzer, A. Leitenstorfer, and G. H. Döhler, Phys. Rev. B **70**, 085211 (2004).
[4] V. Fiorentini, F. Bernardini, F. Della Sala, A. Di Carlo, and P. Lugli, Phys. Rev. B **60**, 8849 (1999).
[5] R. Langer, J. Simon, V. Ortiz, N. T. Pelekanos, A. Barski, R. André, and M. Godlewski, Appl. Phys. Lett. **74**, 3827 (1999).
[6] S.-H. Park and S.-L. Chuang, Appl. Phys. Lett. **76**, 1981 (2000).
[7] A. Hangleiter, F. Hitzel, S. Lahmann, and U. Rossow, Appl. Phys. Lett. **83**, 1169 (2003).
[8] T. Takeuchi, S. Sota, M. Katsuragawa, M. Komori, H. Takeuchi, H. Amano, and I. Akasaki, Jpn. J. Appl. Phys., Part 2 **36**, L382 (1997).
[9] S. P. Łepkowski, T. Suski, P. Perlin, V. Yu. Ivanov, M. Godlewski, N. Grandjean, and J. Massies, J. Appl. Phys. **91**, 9622 (2002).
[10] F. Della Sala, A. Di Carlo, P. Luigi, F. Bernardini, V. Fiorentini, R. Scholz, and J.-M. Jancu, Appl. Phys. Lett. **74**, 2002 (1999).
[11] A. Di Carlo, F. Della Sala, P. Luigi, V. Fiorentini, and F. Bernardini, Appl. Phys. Lett. **76**, 3950 (2000).
[12] D. Turchinovich, P. Uhd Jepsen, B. S. Monozon, M. Koch, S. Lahmann, U. Rossow, and A. Hangleiter, Phys. Rev. B **68**, 241307(R) (2003).
[13] An integral term in Eq. (6) describing the optically induced polarization in the system can be further expressed as $P_{\mathrm{opt}}(t)=eL_z\int_{-\infty}^{t}\Phi(t')\alpha(t')d(t')dt=\chi_{\mathrm{eff}}^{(2)}(t)E^2(t)$, where $\chi_{\mathrm{eff}}^{(2)}(t)$ is the effective time-dependent second-order nonlinear susceptibility, and $E(t)$ is an envelope electric field in the laser pulse. Given $\Phi(t)=I(t)/\hbar\omega=c\varepsilon_0E^2(t)/\hbar\omega$, where $I(t)$ is intensity, one arrives to $\chi_{\mathrm{eff}}^{(2)}(t)=(eL_zc\varepsilon_0/\hbar\omega)\int_{-\infty}^{t}\alpha(t')d(t')dt$. It is obvious that with effective wave-function separation $d(t)$ approaching zero, $\chi_{\mathrm{eff}}^{(2)}$ also vanishes, thus making further polarization buildup impossible.
[14] G. Bastard, E. E. Mendez, L. L. Chang, and L. Esaki, Phys. Rev. B **28**, 3241 (1983).
[15] P. C. M. Planken, M. C. Nuss, W. H. Knox, D. A. B. Miller, and K. W. Goossen, Appl. Phys. Lett. **61**, 2009 (1992).
[16] W. Chow, M. Kira, and S. W. Koch Phys. Rev. B **60**, 1947 (1999).
[17] J. Wagner, H. Obloh, M. Kunzer, M. Maier, K. Köhler, and B. Johs, J. Appl. Phys. **89**, 2779 (2001).
[18] F. Bernardini, V. Fiorentini, and D. Vanderbilt, Phys. Rev. Lett. **79**, 3958 (1997).
[19] H. Schmidt, A. C. Abare, J. E. Bowers, S. P. DenBaars, and A. Imamoglu, Appl. Phys. Lett. **75**, 3611 (1999).
[20] D. Turchinovich, Ph. D. thesis, Freiburg (2004) (available at http://www.freidok.uni-freiburg.de/volltexte/1464/).
[21] P. K. Benicewicz, J. P. Roberts, and A. J. Taylor, J. Opt. Soc. Am. B **11**, 2533 (1994).
[22] C. Kübler, R. Huber, S. Tübel, and A. Leitenstorfer, Appl. Phys. Lett. **85**, 3360 (2004).
[23] G. Gallot and D. Grischkowsky, J. Opt. Soc. Am. B **16**, 1204 (1999).